16th World Conference on Earthquake, 16WCEE 2017

Santiago Chile, January 9th to 13th 2017

Paper N° 424 (Abstract 424)

Registration Code: S-X146123724

NONLINEAR DYNAMIC ANALYSIS OF IN-PLAN IRREGULAR R.C. STRUCTURES RETROFITTED WITH HYSTERETIC DAMPED BRACES

F. Mazza[(1)], E. Pedace[(2)], F. Del Favero[(3)]

[(1)] *Researcher, Dipartimento di Ingegneria Civile, Università della Calabria, Rende (Cosenza), Italy, fabio.mazza@unical.it*
[(2)] *Ph.D., Dipartimento di Ingegneria Civile, Università della Calabria, Rende (Cosenza), Italy, emilia.pedace@unical.it*
[(3)] *Engineer, Dipartimento di Ingegneria Civile, Università della Calabria, Rende (Cosenza), Italy, francescodf86@hotmail.com*

Abstract

The seismic retrofitting of unsymmetric plan reinforced concrete (r.c.) framed buildings can be carried out by the insertion of damped braces (DBs), which are made of steel braces connecting two consecutive storeys and incorporating energy dissipating devices. Yet most of the proposals to mitigate the seismic response of asymmetric framed buildings by DBs rest on the hypothesis of elastic (linear) structural behaviour. The aim of the present work is to evaluate the effectiveness and reliability of a Displacement-Based Design procedure of hysteretic damped braces (HYDBs) based on the nonlinear behaviour of the frame members. An expression of the biaxial viscous damping equivalent to the hysteretic energy dissipated by the damped braced frame is assumed under bidirectional seismic loads, where corrective factors are adopted as a function of design parameters of the HYDBs. Moreover, the extended N2 method considered by Eurocode 8, which combines the nonlinear static analysis along the principal in-plan directions of the structure with elastic modal analysis, is adopted to evaluate the higher mode torsional effects. To this end, the Town Hall of Spilinga (Italy), a reinforced concrete framed structure with an L-shaped plan built at the beginning of the 1960s, is supposed to be retrofitted with HYDBs to attain performance levels imposed by the Italian seismic code (NTC08) in a high-risk zone. Ten structural solutions are compared by considering two alternative in-plan distributions of the HYDBs, to eliminate (elastic) torsional effects, and different design values of the frame ductility combined with a constant design value of the damper ductility. Reinforced concrete (r.c.) structures with asymmetric plan may require the assessment of the critical incident angle of bidirectional ground motions. To this end, a computer code for the nonlinear dynamic analysis of r.c. spatial framed structures is adopted. Frame members are simulated with a lumped plasticity model, including flat surface modelling of the axial load-biaxial bending moment elastic domain, at the end sections of r.c. beams and columns where inelastic deformations generally occur, while a bilinear law is used to idealize the behaviour of a HYDB. Vulnerability index domains of r.c. frame members and HYDBs are adopted to estimate the directions of least seismic capacity, considering artificial ground motions whose response spectra match those adopted by NTC08 at serviceability and ultimate limit states.

Keywords: Unsymmetric-plan framed structures; equivalent biaxial viscous damping; extended N2 method; hysteretic dampers; displacement-based design; nonlinear dynamic analysis.

1. Introduction

The seismic retrofitting of unsymmetric-plan reinforced concrete (r.c.) buildings, one of the most frequently damaged types [1], can be carried out by traditional methods [2] based on conventional materials and construction techniques (e.g. r.c. shear walls, steel braces, steel encasing and concrete jacketing), or modern methods [2] based on new techniques and materials (e.g. added damping, base-isolation and wrapping by means of carbon fiber reinforced polymers). Among the latter, passive control systems based on the incorporation of steel braces connecting two storeys and equipped with displacement- (e.g.: friction damper, FRD; metallic-yielding hysteretic damper, HYD) or velocity-dependent (e.g.: viscoelastic damper, VED; viscous damper, VSD) nonlinear devices represent a cheap and easy solution [3]. In Europe, current seismic codes only implicitly allow for the use of such devices (e.g. European code, EC8 [4]; Italian code, NTC08 [5]), while worldwide very few seismic codes provide for simplified design criteria of DBs (e.g. USA code, FEMA 356 [6]).
Several simplified nonlinear design methods of damped braces (DBs), combining the nonlinear static (pushover) analysis of the multi-degree-of-freedom (MDOF) model of the actual structure with the response spectrum analysis of an equivalent single-degree-of-freedom (ESDOF) system, have been proposed for the seismic retrofitting of regular r.c. framed structures [7]. However, only few design procedures of DBs, based on the nonlinear behaviour of the frame members, have been proposed for an in-plan irregular framed structure [8-10].
The aim of the present work is to evaluate the effectiveness and reliability of a Displacement-Based Design (DBD) procedure of hysteretic damped braces (HYDBs). To this end, a revised expression of the equivalent viscous damping is assumed by considering the hysteretic energy dissipated by a DBF structure under bidirectional seismic loads, where corrective factors are considered as a function of design parameters of the HYDBs [10]. Moreover, the extended N2-method considered by EC8 [4], which adopts correction factors based on elastic modal analysis to evaluate the higher mode torsional effects, is used to improve the nonlinear response obtained by the standard pushover analysis [11].
The case study focus on the Town Hall of Spilinga (Italy), a two-storey r.c. framed structure with an L-shaped plan built at the beginning of the 1960s [10]. This building designed in line with a former seismic code (RDL, 1937 [12]), for a high-risk seismic zone, is retrofitted by the incorporation of HYDBs to attain performance levels imposed by NTC08. To avoid brittle behaviour of the r.c. frame members, different design values of the frame ductility are considered in combination with a constant design value of damper ductility. Moreover, to eliminate (elastic) torsional effects, inversely proportional in-plan stiffness distribution of the HYDBs is assumed. Artificially generated ground motions, whose response spectra match those adopted by the Italian seismic code for different seismic intensity levels, are considered to compare the nonlinear dynamic response of the original and retrofitted structures for different in-plan directions of bidirectional ground motion varying in the range 0-360°, with a constant step of 15°. A lumped plasticity model describes the inelastic behaviour of r.c. frame members, including a 26-flat surface modelling of the axial load-biaxial bending moment elastic domain at the end sections where inelastic deformations are expected [13]; a bilinear model idealizes the nonlinear response of the HYDBs. Vulnerability index domains of r.c. frame members and HYDBs are adopted to evaluate the directions of least seismic capacity at the serviceability and ultimate limit states provided by NTC08.

2. DBD procedure of HYDBs for unsymmetric-plan structures: theory

A DBD iterative procedure of dissipative braces, which is both conceptually clear and simply to apply, is proposed for the seismic retrofitting of in-plan asymmetric r.c. framed structures. More specifically, a six-step DBD design procedure of HYDBs is explained below.

2.1 Extended N2-method for pushover analysis along the principal directions of the in-plan irregular unbraced frame

The aim of the extended N2 method is to take into account the higher mode torsional effects of in-plan irregular framed structures (UF, Fig.1a), by modifying the lowest base shear-top displacement capacity curves ($V^{(F)}$-d) along the X and Y directions. The most common lateral-load profiles are considered for the unbraced frame (UF): e.g. a "uniform" distribution, proportional to the floor masses (m_1, m_2, .., m_n); a “triangular” distribution, obtained by multiplying the first-mode components (ϕ_1, ϕ_2, .., ϕ_n) by the corresponding floor mass. The correction factors, evaluated for each horizontal direction, are defined as the ratio between the normalized top displacements obtained by elastic modal analysis and nonlinear static analysis [11]. The normalized top displacement is defined as the top displacement at an arbitrary in-plan location (e.g. the six corner points shown in Fig. 1a) divided by the corresponding value at the centre of mass (C_M).

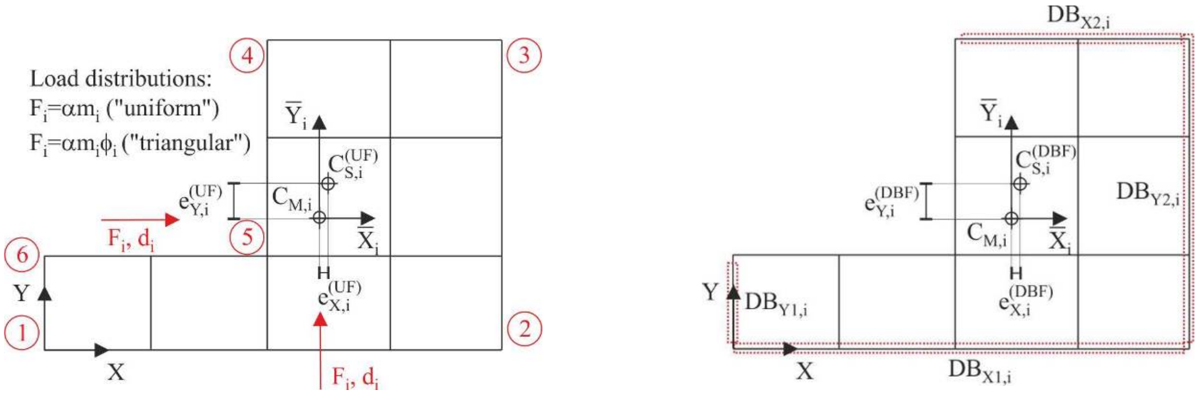

(a) Extended N2-method for the unbraced frame (UF)　　(b) Distribution of HYDBs

Fig. 1 – In-plan irregular framed structure

2.2 Definition of an equivalent two degrees of freedom (ETDOF) system of the unbraced frame (UF) along the principal in-plan directions

The selected $V_\gamma^{(F)}$-d_γ curves ($\gamma\in$(X,Y)) can be idealized as bilinear and the original frame can be represented by an equivalent two degrees of freedom (ETDOF) system characterized by a bilinear curve (V_γ^*-d_γ^*), with a yield displacement $d_{yl,\gamma}^{(F)}$ and a stiffness hardening ratio r_F, derived from the idealized $V_\gamma^{(F)}$-d_γ curve (Fig. 2). Once the displacement ($d_{p,\gamma}$) and the corresponding base shear ($V_{p,\gamma}^{(F)}$) are established, for a given level of performance, the ductility

$$\mu_{F,\gamma} = d_{p,\gamma} \Big/ d_{yl,\gamma}^{(F)} \tag{1}$$

and the equivalent (secant) stiffness

$$K_{e,\gamma}^{(F)} = V_{p,\gamma}^{(F)} \Big/ d_{p,\gamma} \tag{2}$$

can be derived for the frame. Moreover, coefficient of participation (Γ), effective mass (m_e) and effective period ($T_{e,\gamma}$) of the ETDOF system can be evaluated in line with the following expressions:

$$\Gamma = \frac{\sum m_i \phi_i}{\sum m_i \phi_i^2}, \quad m_e = \sum m_i \phi_i \;(\phi_n = 1), \quad T_{e,\gamma} = \frac{2\pi}{\sqrt{m_e \big/ K_{e,\gamma}^{(F)}}} \tag{3a,b,c}$$

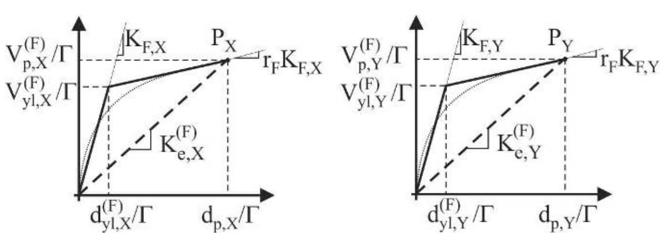

Fig. 2 – Idealized response of the unbraced frame (UF) along the principal in-plan directions

2.3 Biaxial equivalent viscous damping of the equivalent two degrees of freedom (ETDOF) system of the damped braced framed structure (DBF)

The Jacobsen's equivalent viscous damping, equating the energy dissipated per cycle by nonlinear and equivalent linear ETDOF systems, combined with the secant stiffness at maximum displacement are related to the DBD procedure of the HYDBs [10]. Assuming a suitable value of the elastic viscous damping for the framed structure (e.g. ξ_V=5%), the viscous damping of the (linear) elastic ETDOF system (Fig. 3), along the principal in-plan directions ($\gamma \in (X,Y)$), can be evaluated as considering the area (A_1) of a hysteretic loop and the area (A_2) of the rigid-perfectly-plastic loop which encompasses it

$$\xi_{DBF,\gamma} = \xi_V + \frac{2}{\pi}\frac{A_1}{A_2} = \xi_V + \frac{2}{\pi}\left(\xi^{(h)}_{DBF,\gamma 1} + \xi^{(h)}_{DBF,\gamma 2} + \xi^{(h)}_{DBF,\gamma 3}\right) \tag{4}$$

being

$$\xi^{(h)}_{DBF,\gamma 1} = \frac{\mu_{F,\gamma}\left(K^*_\gamma d^*_\gamma + 1 - r_{DB} K^*_\gamma d^*_\gamma\right)}{\mu_{F,\gamma}\left(K^*_\gamma d^*_\gamma + 1 + r_{DB} K^*_\gamma d^*_\gamma (\mu_{DB,\gamma} - 1)\right)} \tag{5a}$$

$$\xi^{(h)}_{DBF,\gamma 2} = \frac{-\dfrac{\left(K^*_\gamma d^*_\gamma + 1 - r_{DB} K^*_\gamma d^*_\gamma\right)^2}{(1 + K^*_\gamma - r_{DB} K^*_\gamma)}}{\mu_{F,\gamma}\left(K^*_\gamma d^*_\gamma + 1 + r_{DB} K^*_\gamma d^*_\gamma (\mu_{DB,\gamma} - 1)\right)} \tag{5b}$$

$$\xi^{(h)}_{DBF,\gamma 3} = \frac{\dfrac{\left(1 - d^*_\gamma\right)}{2}\left(\dfrac{K^*_\gamma d^*_\gamma + 1 - r_{DB} K^*_\gamma d^*_\gamma}{1 + K^*_\gamma - r_{DB} K^*_\gamma} - 1\right)}{\mu_{F,\gamma}\left(K^*_\gamma d^*_\gamma + 1 + r_{DB} K^*_\gamma d^*_\gamma (\mu_{DB,\gamma} - 1)\right)} \tag{5c}$$

where r_{DB} is the stiffness hardening ratio of the HYDB while

$$K^*_\gamma = K_{DB,\gamma} / K_{F,\gamma}, \quad d^*_\gamma = d^{(DB)}_{yl,\gamma} / d^{(F)}_{yl,\gamma} \tag{6}$$

are the stiffness and the displacement ratios, respectively, and

$$\mu_{DB,\gamma} = d_{p,\gamma} / d^{(DB)}_{yl,\gamma} \tag{7}$$

is the ductility demand of the YL damped brace (DB).

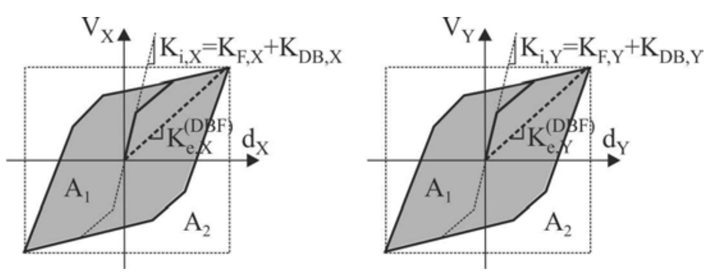

Fig. 3 – Idealized response of the damped braced frame (DBF) along the principal in-plan directions

Finally, it can be shown that the elastic ETDOF system has effective period

$$T_{e,\gamma} = T_{i,\gamma}\sqrt{\frac{\mu_{F,\gamma} + K^*_\gamma d^*_\gamma \mu_{DB,\gamma}}{1 + K^*_\gamma d^*_\gamma + r_{DB} K^*_\gamma \left(\mu_{F,\gamma} - d^*_\gamma\right)}} \tag{8}$$

shifted in comparison with the initial period of the inelastic (trilinear) ETDOF system

$$T_{i,\gamma} = 2\pi \sqrt{\frac{m_e}{K_{F,\gamma} + K_{DB,\gamma}}} \tag{9}$$

along the principal in-plan directions ($\gamma \in (X,Y)$). Then, a revised relationship for the viscous damping equivalent to the hysteretic energy dissipation of the damped braced frame is proposed

$$\overline{\xi}_{DBF,\gamma} = C_\gamma \xi_{DBF,\gamma} \tag{10}$$

where corrective factor

$$C_\gamma = 0.047 K_\gamma^* + 0.028 d_\gamma^* + 0.416 \tag{11}$$

is evaluated as a function of the design parameters (i.e. K^*_γ, d^*_γ and r_{DB}**)** of HYDBs [10]. Finally, the equivalent (viscous) biaxial damping ratio can be computed

$$\xi_{e,DBF} = \left(E_{S,x}\overline{\xi}_{DBF,x} + E_{S,y}\overline{\xi}_{DBF,y}\right) \Big/ \left(E_{S,x} + E_{S,y}\right) \tag{12}$$

by considering the effective damping for each direction weighted by the corresponding potential energy [14]:

$$E_{S,\gamma} = 0.5 K_{e,\gamma}^{(DBF)} d_{p,\gamma}^2 \tag{13}$$

2.4 Effective stiffness of the equivalent damped braces along the principal in-plan directions

Once the mass (m_e) and period ($T_{e,\gamma}$) of the ETDOF system are calculated, the effective stiffness of the DBF structure ($K_{e,\gamma}$) and the effective stiffness required by dissipative braces (i.e. $K_{e,\gamma}^{(DB)}$ in Fig. 4) can be evaluated along the principal directions ($\gamma \in (X,Y)$):

$$K_{e,\gamma} = 4\pi^2 m_e \big/ T_{e,\gamma}^2, \quad K_{e,\gamma}^{(DB)} = K_{e,\gamma} - K_{e,\gamma}^{(F)} \tag{14a,b}$$

2.5 Effective strength of the equivalent damped braces along the principal in-plan directions

Since the base shear-displacement curve representing the response of the dissipative braces of the actual structure ($V_\gamma^{(DB)}$-d_γ) has been idealized as bilinear (Fig. 4), the base-shear contributions of the damped braces at the performance and yielding points ($V_{p,\gamma}^{(DB)}$ and $V_{yl,\gamma}^{(DB)}$, respectively) can be calculated along the principal directions ($\gamma \in (X,Y)$):

$$V_{p,\gamma}^{(DB)} = K_{e,\gamma}^{(DB)} d_{p,\gamma}, \quad V_{yl,\gamma}^{(DB)} = V_{p,\gamma}^{(DB)} \Big/ \left[1 + r_{DB}\left(\mu_{DB,\gamma} - 1\right)\right] \tag{15a,b}$$

It is worth noting that the equivalent biaxial viscous damping expressed by Eq. (12) depends on the effective stiffness of DBF ($K_{e,\gamma}$), which is initially unknown. Thus, an iterative procedure is needed for the solution of Eqs. (12)-(15).

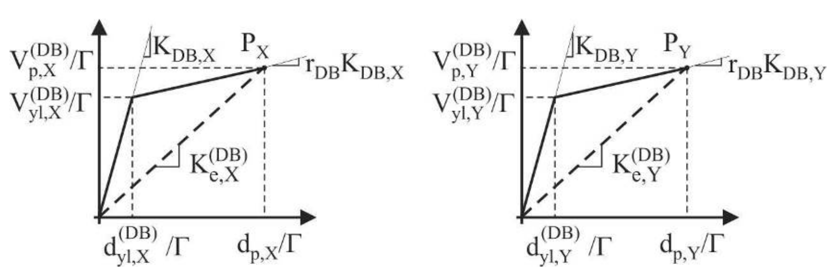

Fig. 4 – Idealized response of the damped braces (DBs) along the principal in-plan directions

2.6 Design of the HYDBs of the damped braced frame (DBF)

Once the in-elevation distribution of the lateral loads carried by the HYDBs at the yielding point ($d_{y,\gamma}^{(DB)}$) is evaluated:

$$V_{yli,\gamma}^{(DB)} = \sum_{j=i}^{n} F_{ylj,\gamma}^{(DB)} = \sum_{j=i}^{n} \frac{m_j \phi_j}{\sum_{k=1}^{n} m_k \phi_k} V_{yl,\gamma}^{(DB)} \tag{16}$$

the corresponding lateral stiffness of the HYDBs, at the i[th] storey, can be obtained along the principal directions:

$$K_{i,\gamma}^{(DB)} = V_{yli,\gamma}^{(DB)} \Big/ \left[\left(\phi_i - \phi_{i-1} \right) d_{yl,\gamma}^{(DB)} \right] \tag{17}$$

Afterwards, the in-plan stiffness distribution of the HYDBs is assumed in accordance with an inversely proportional criterion, which considers a position of the centre of stiffness of the damped braced frame (i.e. $C_{S,i}$ in Fig. 1b) equal to that of $C_{M,i}$ (i.e. assuming $e_{X,i}^{(DBF)}=e_{Y,i}^{(DBF)}=0$) to eliminate (elastic) torsional effects. The following two linear systems are required for X and Y directions:

$$\begin{cases} \dfrac{K_{X1}^{(DB)} \overline{Y}_1^{(DB)} + K_{X2}^{(DB)} \overline{Y}_2^{(DB)}}{K_{X1}^{(DB)} + K_{X2}^{(DB)} + \sum_{j=1}^{n_{FX}} K_{Xj}^{(F)}} = e_Y^{(DBF)} \\ K_{X1}^{(DB)} + K_{X2}^{(DB)} = K_{i,X}^{(DB)} \end{cases} , \quad \begin{cases} \dfrac{K_{Y1}^{(DB)} \overline{X}_1^{(DB)} + K_{Y2}^{(DB)} \overline{X}_2^{(DB)}}{K_{Y1}^{(DB)} + K_{Y2}^{(DB)} + \sum_{j=1}^{n_{FY}} K_{Yj}^{(F)}} = e_X^{(DBF)} \\ K_{Y1}^{(DB)} + K_{Y2}^{(DB)} = K_{i,Y}^{(DB)} \end{cases} \tag{18a,b}$$

3. DBD procedure of HYDBs for unsymmetric-plan structures: application

The test structure is a two-storey r.c. framed structure, with an L-shaped irregular plan (Fig. 5a), built at the beginning of the 1960s to comply with the admissible tension method, for a high-risk seismic region (degree of seismicity S=12, corresponding to a coefficient of seismic intensity C=0.10) and a medium subsoil class, in line with the Royal Decree-Law in 1937 [12]. For a better understanding of the Spilinga Town Hall (Vibo Valentia Italy), the present work uses a simulated design, with reference to the 1937 RDL and to the seismic classification available at the time of construction [10]. Section dimensions of columns (c), constant along the two storeys, and deep (d) and flat (f) beams are reported in Fig. 5b and Table 1.

(a) Current state

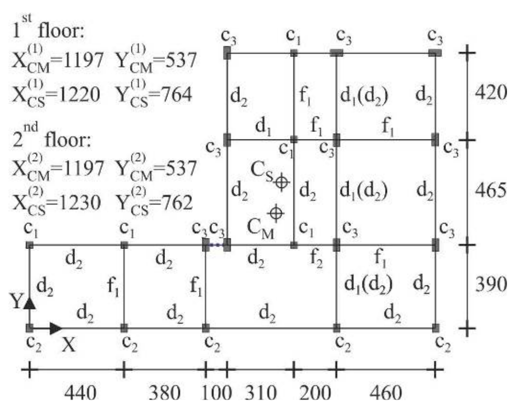

(b) Typologies of cross-section

Fig. 5 - Town Hall of Spilinga (Vibo Valentia, Italy)

Table 1 – Cross-section of columns (c) and deep (d) and flat (f) beams (units in cm)

c_1	c_2	c_3	d_1	d_2	f_1	f_2
30x30	30x40	30x60	30x40	35x50	60x21	90x21

The gravity loads are represented by dead and live loads, whose values are, respectively, equal to: 5.1 kN/m^2 and 3 kN/m^2, on the first floor; 3.9 kN/m^2 (including also the weight of the roof) and 0.5 kN/m^2, on the second floor. The contribution of the masonry-infills is taken into account by considering a weight of 2.7 kN/m^2. Concrete cylindrical compressive strength of 16.6 N/mm^2 and steel reinforcement yield strength of 310 N/mm^2 are divided by a confidence factor of 1.2. The total mass of the building is equal to 458 tons, subdivided between 268 tons and 190 tons on the first and second floor, respectively. The position of the mass and stiffness centres is plotted in Fig. 5b on the first (i.e. $C_{M,1}$ and $C_{S,1}$) and second (i.e. $C_{M,2}$ and $C_{S,2}$) floor. In Table 2, dynamic properties are reported for the two translational modes, along the main axes in plan, and the torsional mode, around the vertical axis: i.e. the vibration period (T); the effective modal masses in the X (i.e. $m_{E,X}$) and Y (i.e. $m_{E,Y}$) directions, expressed as percentages of the total mass (m_t) of the structure.

Table 2 - Dynamic properties of the test structure (m_t= m_1+m_2= 268 +190 = 458 ton)

Vibration mode	**T (s)**	**$m_{E,X}$ (%m_t)**	**$m_{E,Y}$ (%m_t)**
1	0.42	73.9	3.5
2	0.30	3.5	36.9
3	0.35	15.2	49.8

For the purpose of retrofitting the original structure into line with the provisions imposed by NTC08 [5], assuming a high-risk seismic region (peak ground acceleration on rock, a_g=0.306g) and soft subsoil class (subsoil parameter, S=1.275), diagonal steel braces equipped with HYDs are inserted. HYDBs are placed along the in-plan directions only in the perimeter plane frames (i.e. case A in Fig. 6a) and in the perimeter and interior plane frames (i.e. case B in Fig. 6b). The position of the mass and stiffness centres on the floor levels is also plotted in Fig. 6, where cases A and B are designed to eliminate (elastic) torsional effects.

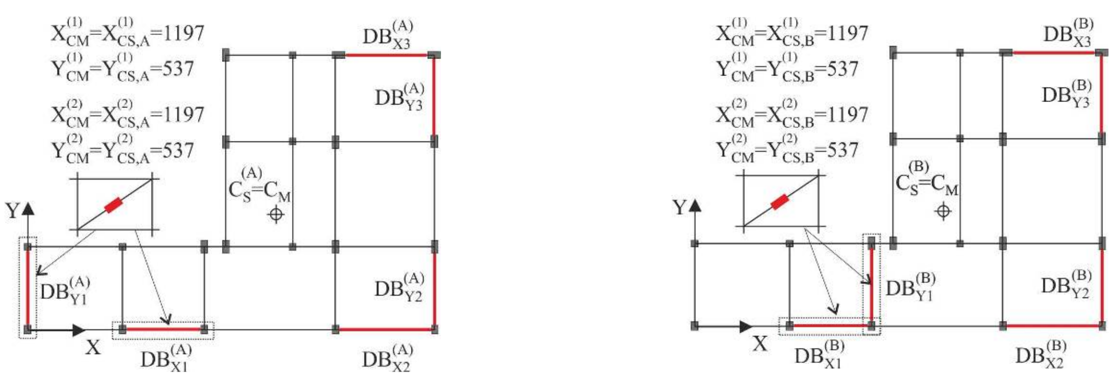

(a) Case A (b) Case B

Fig. 6 - In-plan distribution of DBs (units in cm)

To avoid brittle behaviour at the life-safety (LS) limit state, five design solutions are considered: subcases n.1, n.2, n.4 and n.5 consider equal design values of μ_F in the X and Y directions (i.e. μ_{F1}=1.8=1.5*γ_{SLV}, μ_{F2}=2.4 =1.5*γ_{SLV}, μ_{F4}=μ_{F5}=1.2=1.0*γ_{SLV}, being γ_{SLV}=1.2 a safety factor); subcase n.3 assumes different design values of the frame ductility (μ_F) in the X and Y directions (i.e. $\mu_{F3,X}$=0.7$\mu_{Fu,X}$=2.8 and $\mu_{F3,Y}$=0.7$\mu_{Fu,Y}$=3.2). In the subcases n1-n.4, a design value of the damper ductility μ_D=20 and a hardening ratio r_D=5% are assumed for all the HYDs, both values verified experimentally. Finally, the fifth design solution (i.e. subcase n.5) is characterized by a different hardening ratio (i.e. r_D=2%) for the HYDs. Note that the (elastic) lateral stiffness of the dissipative brace (K_{DB}) is assumed equal to the lateral stiffness of the damper (K_D), given that the brace is much stiffer than the damper it supports (i.e. $K_B\rightarrow\infty$); analogous assumption is adopted for the stiffness hardening ratio (i.e. r_{DB}=r_D). In-plan and in-elevation laws of stiffness (i.e. $K_i^{(DB)}$) and yield-load (i.e. $N_{yl,i}^{(DB)}$) of the HYDBs, in the diagonal direction, are reported in Tables 3 and 4, respectively. Strength distribution of the

HYDBs is assumed proportional to the stiffness distribution.

Table 3. Diagonal stiffness of the HYDBs in the X and Y directions (dimensions in kN/m)

Case	Storey	X_1	X_2	X_3	Y_1	Y_2	Y_3
A.1	1	569579	569579	626788	695964	204898	204898
	2	364147	364147	327485	401460	124905	124905
A.2	1	417898	417898	428085	490992	146182	146182
	2	274061	274061	208226	280792	90285	90285
A.3	1	350766	350766	340140	359904	108630	108630
	2	234189	234189	155444	203619	68144	68144
A.4	1	936613	936613	1107607	1205422	350838	350838
	2	582136	582136	616063	701382	210955	210955
A.5	1	1278491	1278491	1555470	1660213	481118	481118
	2	785183	785183	884862	969120	287771	287771
B.1	1	569579	569579	626788	378611	361923	361923
	2	364147	364147	327485	208303	220627	220627
B.2	1	417898	417898	428085	264581	258209	258209
	2	274061	274061	208226	141173	159475	159475
B.3	1	350766	350766	340140	191654	191880	191880
	2	234189	234189	155444	98240	120366	120366
B.4	1	936613	936613	1107606	662033	619705	619705
	2	582135	582135	616063	375156	372621	372621
B.5	1	1278491	1278491	1555470	915043	849825	849825
	2	785183	785183	884862	524104	508305	508305

Table 4. Diagonal strength of the HYDBs in the X and Y directions (dimensions in kN)

Case	Storey	X_1	X_2	X_3	Y_1	Y_2	Y_3
A.1	1	289	269	296	472	139	137
	2	168	158	142	251	78	77
A.2	1	283	263	269	444	132	131
	2	168	158	120	234	75	75
A.3	1	281	261	253	429	130	128
	2	170	160	106	224	75	74
A.4	1	317	295	349	545	159	157
	2	179	169	178	293	88	87
A.5	1	433	403	490	750	217	215
	2	242	227	256	404	120	119
B.1	1	289	269	296	257	246	244
	2	168	158	142	131	138	137
B.2	1	283	263	269	240	234	232
	2	168	158	120	118	133	132
B.3	1	281	261	253	229	230	227
	2	170	160	106	109	133	132
B.4	1	317	295	349	300	281	278
	2	179	169	178	157	156	155
B.5	1	433	403	490	415	385	381
	2	242	227	256	219	213	211

4. Numerical results

A numerical investigation is carried out to assess the effectiveness and reliability of the DBD design procedure of HYDBs proposed for seismic retrofitting of framed structures with unsymmetric-plan. The nonlinear dynamic analysis of the Spilinga building is carried out for different in-plan directions of bidirectional ground motions (varying in the range 0°-360°, with a constant step of 15°). A piecewise linearization of the axial load-biaxial bending moment ultimate domain, obtained by considering 26 flat surfaces, is considered for cross-sections, while a lumped plasticity model constituted of two parallel elements, one linearly elastic and the other elastic-perfectly plastic, is considered to describe the inelastic behaviour of r.c. frame members [13]. Moreover, the behaviour of a HYDB is idealized through a bilinear law assuming that yielding and buckling are prevented for the steel braces supporting the HYDs. Two sets of three artificial motions, generated by the computer code SIMQKE [15], are considered for serviceability (i.e. operational, OP) and ultimate (i.e. life-safety, LS) limit states provided by NTC08 [5]. The response spectra of these artificial accelerograms match, on average, NTC08 spectra for subsoil class D and the geographical coordinates (i.e. longitude 15.91° and latitude 38.63°). Moreover, each motion, with a duration of 20 s, is generated as to be stationary in frequency in the range of vibration periods 0.05s-4s, with a PGA value close to that of the corresponding target NTC08 spectrum: i.e., PGA_{OP}=0.20g and PGA_{LS}=0.39g.

Firstly, the storey damage at the OP and LS limit states is shown in Figs. 7 and 8, respectively, for the the original (UF) and retrofitted (DBF) structures, with reference to the maximum values of interstorey drift ratio, defined as drift normalized by the storey height. Moreover, drift ratio thresholds related to moderate-damage (Fig. 7) and life-safety (Fig. 8) levels are also reported [16].

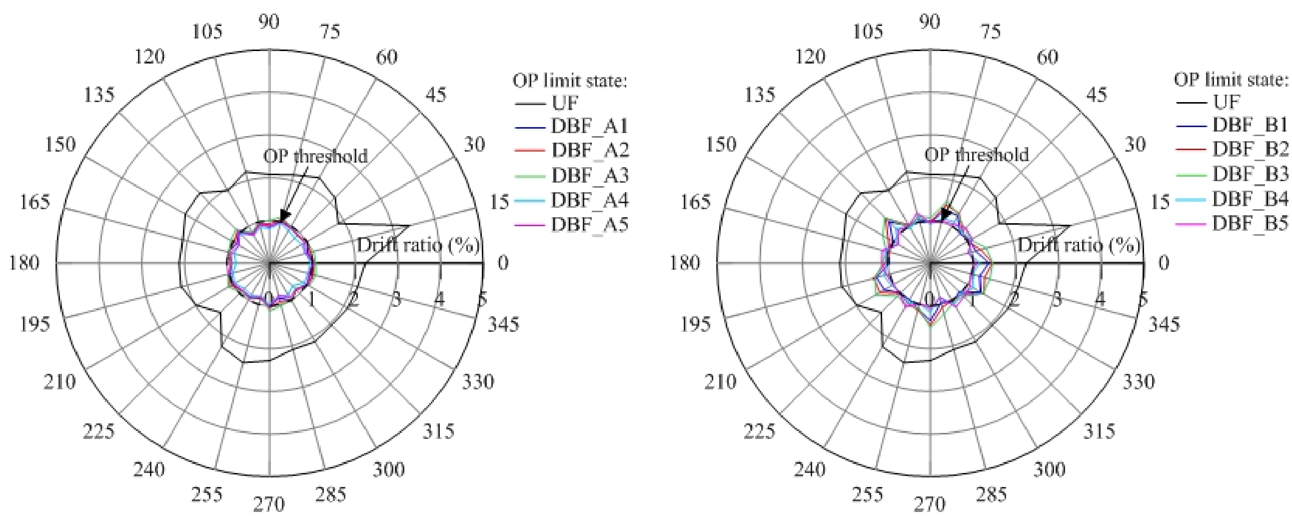

(a) (b)

Fig. 7 – Maximum interstorey drift ratio at OP limit state, assuming two in-plan distributions (cases A and B) of HYDBs

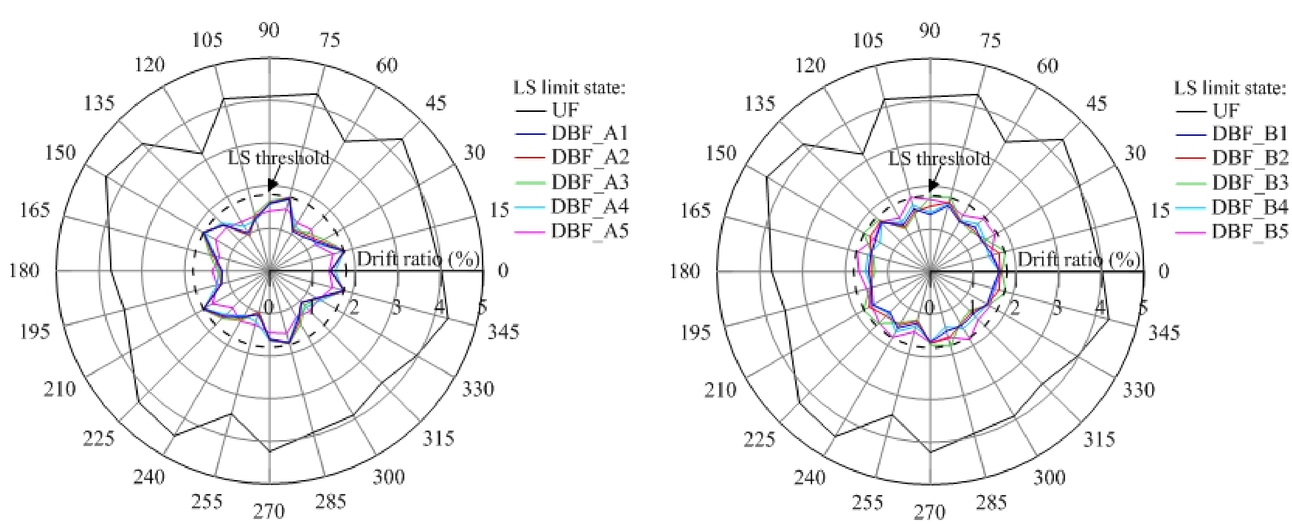

(a) (b)

Fig. 8 – Maximum interstorey drift ratio at LS limit state,
assuming two in-plan distributions (cases A and B) of HYDBs

Two stiffness distributions of the HYDBs (i.e. DBF_A and DBF_B cases shown in Figs. 6a and 6b, respectively) are compared. It is worth noting that the least seismic capacity directions for the unbraced frame (UF), whose response is plotted with a solid black line, are not necessarily the same at the serviceability and ultimate limit states. Moreover, the UF structure has clearly exceeded the vulnerability threshold at both OP and LS limit states, showing an irregular shape of the corresponding drift ratio domains. The results highlight the fact that DBF_A and DBF_B structures, which are retrofitted for the LS limit state, also work well for the OP limit state. In particular, the insertion of the HYDBs generally reduces the maximum values of drift ratio below the OP (Fig. 7a) and LS (Figs. 8a,b) thresholds, confirming the effectiveness of their design for limiting storey damage. Moreover, the shape of the drift ratio domains obtained for the DBF_B (Fig. 8b) proves to be more regular than that observed for the DBF_A (Fig. 8a), at the LS limit state. The numerical results also show that the responses of the structures with different design values of frame ductility, but the same value of HYDBs ductility, respond in a similar way for different in-plan directions of the seismic loads. Finally, it is interesting to note that the most vulnerable seismic direction is not necessarily the same for the DBF_Ai and DBF_Bi (i=1-5) structures.

Curves analogous to those above are plotted in Fig. 9 to compare the maximum residual drift ratio obtained for the unbraced (UF) and damped braced frames (DBFs), considering the LS limit state. The residual drift ratio is an important parameter because it represents the irrecoverable part of the interstorey drift, related to damage requiring repair after an earthquake. Note that a highly irregular shape of the residual drift ratio domain is obtained for the UF structure, while the re-centering of the HYDBs proves to be very effective for both the DBF_A and DBF_B structures. Moreover, in terms of residual drift ratio the least seismic capacity directions do not necessarily coincide with those obtained above in terms of maximum drift ratio.

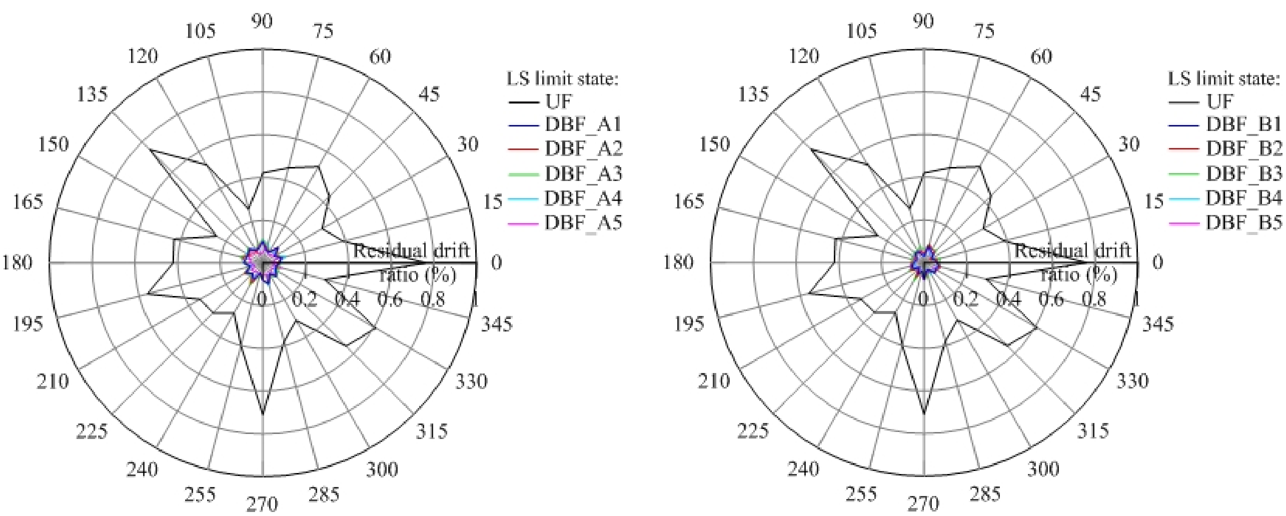

(a) (b)

Fig. 9 – Maximum residual interstorey drift ratio at LS limit state,
assuming two in-plan distributions (cases A and B) of HYDBs

Next, local structural damage along the building height, in terms of maximum curvature ductility demand at the end sections of columns, is shown in Fig. 10. In detail, the ductility demand is evaluated with reference to the radial direction, this being sensitive to the direction of the bending moment axis vector, which changes at each step of the loading process. A strong beams-weak columns mechanism is highlighted for the UF structure, with high ductility demand in the columns, for all direction of the seismic loads. As can be observed, the insertion of the HYDBs is effective in reducing the ductility demand at the LS ultimate limit state. Similar results are obtained for all the examined solutions (i.e. subcases n.1-n.5), further confirming the reliability and robustness of the proposed design procedure.

Afterwards, maximum ductility demand of HYDBs in the DBF_A and DBF_B structures is plotted in Fig.

11, assuming different design values of the frame ductility (i.e. subcases n.1-n.4) and hardening ratio of the damper (i.e. subcases n.4 and n.5). As expected, the damper ductility demand increases for decreasing values of μ_F: i.e. the DBF_A3 and DBF_B3 structures manifest higher values of $\mu_{D,max}$ than the DBF_A1 and DBF_A2 (Fig. 11a) and DBF_B1 and DBF_B2 (Fig. 11b) structures, respectively. On the other hand, the damper ductility demand decreases for decreasing values of r_D. However, in all the examined cases the ductility threshold of the HYDBs (i.e. μ_D=20) is not reached for all the in-plan directions of the seismic loads.

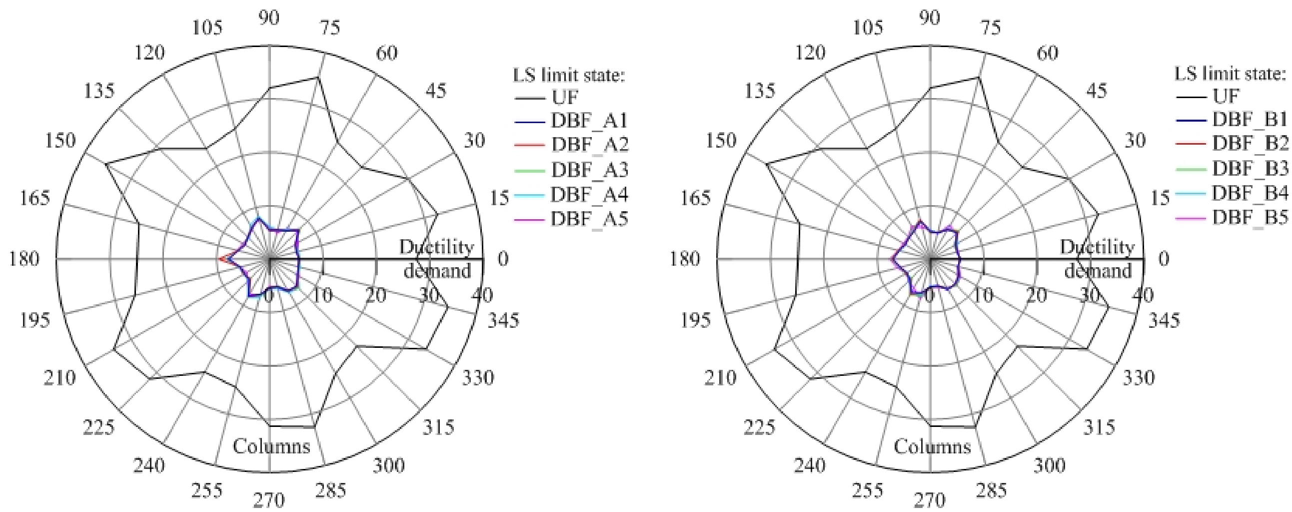

(a) (b)

Fig. 10 – Maximum ductility demand of columns at LS limit state, assuming two in-plan distributions (cases A and B) of HYDBs

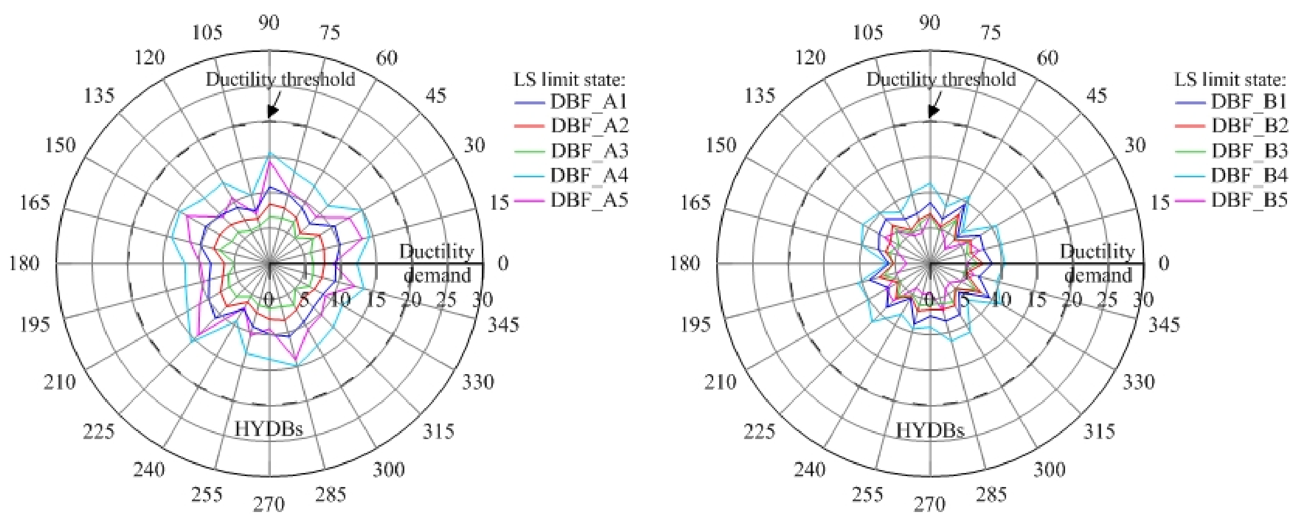

(a) (b)

Fig. 11 – Maximum ductility demand of HYDBs at LS limit state, assuming two in-plan distributions (cases A and B)

5. Conclusions

A Displacement-Based Design procedure of HYDBs is proposed for the seismic retrofitting of in-plan irregular r.c. framed buildings, which is consistent with the extended N2 method enveloping the results of basic pushover analysis and standard elastic modal analysis. Ten structural solutions for retrofitting the Town Hall of Spilinga (Italy) are compared, assuming two in-plan distributions of HYDBs, to eliminate (elastic) torsional effects in the DBF structure, four design values of the frame ductility and two design values of the damper hardening ratio.

Nonlinear dynamic analyses are carried out with a lumped plasticity describing the inelastic behaviour of beams and columns, including 26-flat surface modelling of the axial load-biaxial bending moment elastic domain at the end sections where inelastic deformations are expected, and a bilinear model to idealize the nonlinear response of the HYDBs. The maximum drift ratio, well correlated with the storey structural damage, confirms that DBF_A and DBF_B structures, which are retrofitted for the LS limit state, also work well for the OP limit state. Moreover, the most vulnerable seismic direction is not necessarily the same at serviceability and ultimate limit states. An irregular shape of the residual drift ratio domain, representing the irrecoverable part of the interstorey drift, is obtained for the UF structure, while re-centering capabilities of the HYDBs proves to be very effective for both the DBF_A and DBF_B structures. The insertion of HYDBs is effective in reducing the local structural damage at the LS limit state, in terms of maximum curvature ductility demand at the end sections of columns. As further confirmation of the reliability and robustness of the design procedure, comparable results are obtained for different configurations of HYDBs, whose ductility demand does not exceed the design threshold.

6. Acknowledgements

The present work was financed by ReLUIS (Italian network of university laboratories of earthquake engineering), in accordance with “Convenzione DPC–ReLUIS 2014–2016, WPI, Isolation and Dissipation”.

7. References

[1] Anagnostopoulos SA, Kyrkos MT, Stathopoulos KG (2015): Earthquake induced torsion in buildings: critical review and state of the art. *Earthquakes and Structures*, **8**(2), 305-377.

[2] Calvi GM (2013): Choices and criteria for seismic strengthening. *Journal of Earthquake Engineering*, **17**(6), 769-802.

[3] Christopoulos C, Filiatrault A (2006): *Principles of passive supplemental damping and seismic isolation*. IUSS Press, Istituto Universitario di Studi Superiori di Pavia, Italy.

[4] Eurocode 8 (2003): Design of structures for earthquake resistance - part 1: general rules, seismic actions and rules for buildings. C.E.N., European Committee for Standardization.

[5] NTC08 (2008): Technical Regulations for the Constructions. Italian Ministry of the Infrastructures (in Italian).

[6] Federal Emergency Management Agency, FEMA 356 (2000): Prestandard and commentary for the seismic rehabilitation of buildings. American Society of Civil Engineers, Reston, Virginia.

[7] REte dei Laboratori Universitari di Ingegneria Sismica (2014): Linee guida di progettazione per strutture con sistemi di dissipazione di energia: esempi applicativi. *Report DPC-RELUIS*, **1**, 1-168 (in Italian).

[8] Fujii K (2015): Application of the pushover-based procedure to predict the largest peak response of asymmetric buildings with buckling-restrained braces. *COMPDYN 2015, 5th ECCOMAS Thematic Conference on Computational Methods in Structural Dynamics and Earthquake Engineering*, Crete, Greece, May 25–27, paper n. 836.

[9] Goel RK (2005): Seismic response of linear and non-linear asymmetric systems with non-linear fluid viscous dampers. *Earthquake Engineering and Structural Dynamics*, **34**(7), 825-846.

[10] Mazza F (2016): Nonlinear seismic analysis of unsymmetric-plan structures retrofitted by hysteretic damped braces *Bulletin of Earthquake Engineering*, **14**, 1311-1331.

[11] Kreslin M, Fajfar P (2012): The extended N2 method considering higher mode effects in both plan and elevation. *Bulletin of Earthquake Engineering*, **10**, 695-715.

[12] Royal Decree-Law No. 2105 (1937): Technical Building Regulations, with special prescriptions for localities affected by earthquakes (in italian).

[13] Mazza F (2014): Modeling and nonlinear static analysis of reinforced concrete framed buildings irregular in plan. *Engineering Structures*, **80**, 98-108.

[14] Rodrigues H, Varum H, Arêde A, Costa A (2012): A comparative analysis of energy dissipation and equivalent viscous damping of RC columns subjected to uniaxial and biaxial loading. *Engineering Structures*, **35**, 149-164.

[15] Gasparini D, Vanmarcke E (1976): Simulated earthquake motions compatible with prescribed response spectra. *Massachusetts Institute of Technology, Department of Civil Engineering*, U.S.A..

[16] Ghobarah A (2004): On drift limits associated with different damage levels. *Procs. of the International Workshop Performance-Based Seismic Design: Concepts and Implementation*, Bled, Slovenia, 2004.